Energy Spectra and Level Densities From Inelastic Proton Scattering

H. Nann and J.A. Nolen

High resolution (2-3 keV) inelastic proton scattering allows the determination of very accurate excitation energies. The uncertainties assigned to these excitation energies are on the order of 0.2 - 1.0 keV. The precision is comparable to that of typical γ-ray measurements up to 3 MeV of excitation and often superior at higher energies. In addition, the low- and high-excitation energy level schemes can be simultaneously established unambiguously. Finally, this reaction is well suited to yield a complete catalogue of excited states.

The density of levels near the threshold of particle emission is presently needed for the evaluation of the response of various isotopes to bombardment with neutrons in reactors. The main source of information on nuclear level densities has been experiments on the resonant capture of slow neutrons. Since the penetrability of these neutrons decreases rapidly with increasing angular momentum, only low-spin resonances are excited with reasonable strength. An alternative method by which to obtain data on such level densities is to study inelastic proton scattering with very good energy resolution.

Inelastic proton scattering on ^{31}P, ^{58}Ni and ^{60}Ni have been performed at a bombarding energy of 35 MeV. The spectra were recorded in nuclear emulsions in the focal plane of the Enge split-pole magnetic spectrograph. An experimental resolution of 2.5 keV, full width at half maximum was obtained by using the spectrometer in the energy-loss, or dispersion-matching, mode. The resolution was measured and optimized using the on-line tuning procedure described in ref. 1. The resulting spectra are nearly completely free from background.

Figure 1 shows a spectrum from the $^{31}P(p,p')$ reaction. About 250 levels are excited in range of excitation energy 0 - 11 MeV. The excitation energies of the levels below 8 MeV were determined with an uncertainty of 0.2 - 0.4 keV depending on the uncertainties of the calibration lines. Because of the lack of well-known calibration lines for the higher excitation energy region, the accuracy of the excitation assignments for states above 8 MeV range between 1 and 2 keV. Efforts are under way to establish better calibration lines for this excitation energy region.

From such data level densities can be determined in the most direct way, by simply counting the number of levels per energy interval. However, two kinds of systematic errors will have to be considered before numbers so obtained can be compared to any theoretical prediction, namely that some levels will escape detection due to their low cross section, and that some closely spaced levels will still remain unresolved.

References

1. H.G. Blosser et al., Nucl. Instr. Methods, 91 1(1971).

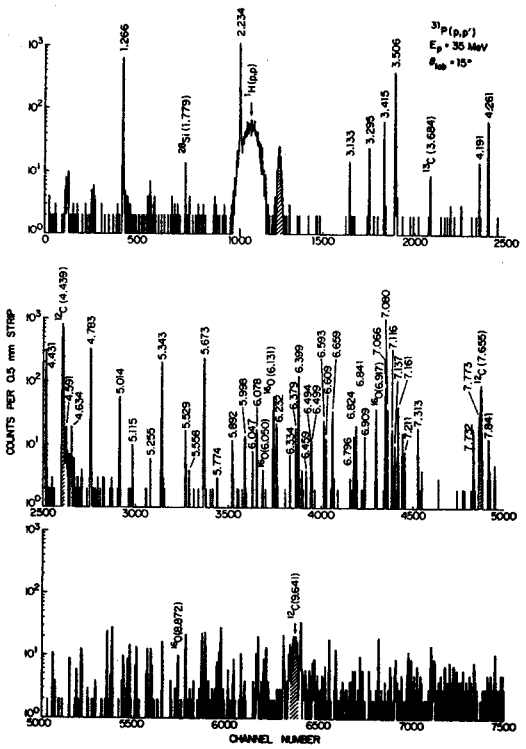

Figure 1.--Spectrum of the $^{31}P(p,p')$ reaction at a scattering angle of 15° and a bombarding energy of 35 MeV.

Nuclear Deformation Measurements via (p,p') Reactions

G.C. Crawley, J.E. Finck, C.H. King, and J.A. Nolen,Jr.

We have initiated a study of the (p,p') reaction on rare earth and actinide nuclei at a beam energy of 35 MeV. To date we have recorded angular distributions from 20°to 120° scattering angles on targets of ^{154}Sm, ^{176}Yb, ^{232}Th, and ^{238}U. Data have been obtained with a position sensitive proportional counter (8-10 keV FWHM) and with nuclear emulsions (5 keV FWHM).

The analysis so far has been concentrated on fitting the angular distributions of the ground state rotational band. Good data have been obtained for the 0^+, 2^+, 4^+, 6^+, and sometimes 8^+ members of this band. The qualitative results are that the angular distributions are much more structured than either those from (p,p') reactions on spherical nuclei or on deformed nuclei at lower bombarding energies (∿23 MeV or less), an observation which can be accounted for by coupled channels calculations including interference between direct and multiple step excitation of the 0^+, 2^+, 4^+, 6^+ states. Indeed, it is possible to fit the angular distributions for the 0^+, 2^+, and 4^+ states by varying β_2, β_4, and β_6 nuclear deformation parameters in the rotational model. These angular distributions are very sensitive to the magnitude and signs of the β_2 and β_4 parameters. The detailed fits to the 6^+ angular distributions are not nearly as good as those to the first 3 members of the band. Calculations including deformed spin-orbit potential contributions are currently being run to see if they may be the cause of this problem. A preliminary calculation limited to the first 3 levels has shown the spin-orbit force to have no major effect on the 0^+, 2^+, and 4^+ angular distributions.

Our results on the deformation parameters are not completely consistent with existing measurements on these nuclei. For example, using the values of β_2, β_4, and β_6 properly scaled from the (α,α') work of Hendrie, et al. at 50 MeV together with Becchetti-Greenlees global optical model parameters (i.e. a parameter free calculation) produced a good fit to the ^{154}Sm and ^{238}U data, but did not do well for the ^{176}Yb. For ^{176}Yb we prefer a 10% larger β_2 and over 50% more negative β_4 than Hendrie, et al. It is interesting to note that fits to (e,e') data on ^{176}Yb seem to require a mass distribution that is not a pure deformed Fermi shape.

Since the (p,p') data at these higher energies do determine a set values of β_2, β_4, and β_6 for each nucleus, we will continue these experiments on other deformed and transitioned nuclei to map out the trends in these deformation parameters. The comparison of results to (α,α'), Coulomb excitation, Coulomb-nuclear interference, and (e,e') results may be illuminating. Questions to be addressed include the relationship between the charge deformation parameters and the nuclear potential well deformations, as well as effects due to differences in proton and neutron deformations.

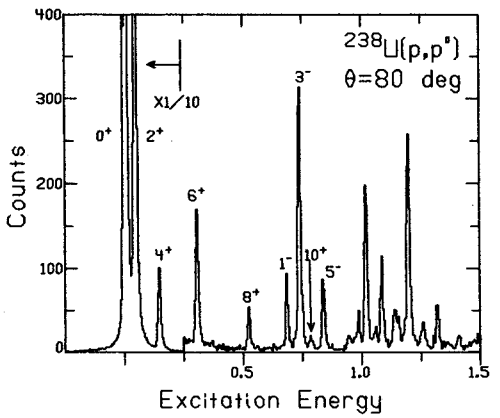

Fig. 1 Spectrum of protons inelastically scattered from ^{238}U.

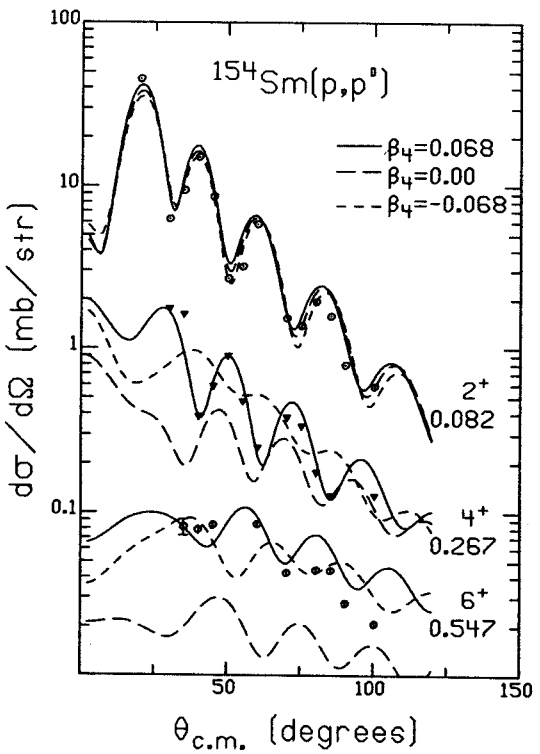

Fig. 2. Coupled channels distorted wave calculations compared with the data from $^{154}Sm(p,p')$. The curves show that the calculations are very sensitive to the value of β_4.

Particle-hole States in ^{28}Si

H. Nann, J.A. Nolen, J. Finck, J. van Hienen, and G.M. Crawley

Unnatural parity particle-hole states are of particular interest in (p,p') reactions because they are populated through poorly known components of the nucleon-nucleon force, e.g., the tensor and spin-orbit interactions. However, there are relatively few such states known which can be used to test microscopic (p,p') calculations. Candidates for 6^- and 4^- states in ^{28}Si at 13-15 MeV excitation have been reported an (e,e') experiment.[1]

To further establish the particle-hole nature of these states we have measured angular distributions of the $^{27}Al(^3He,d)^{28}Si$ reaction at 35 MeV. We have also measured $^{28}Si(p,p')$ at 40 MeV to see if these states are populated in this reaction. By inelastic proton scattering one-particle, one-hole states of all possible configurations can be excited, whereas in the $^{27}Al(^3He,d)$ reaction only those states with a $1d_{5/2}$ hole and particles in the $2s_{1/2}$, $1d_{3/2}$, $1f_{7/2}$, $2p_{3/2}$...orbitals are expected to show up strongly.

Figure 1 shows a $^{28}Si(p,p')$ and a $^{27}Al(^3He,d)$ spectrum. The abscissa of both spectra are presented such that peaks corresponding to the same excitation energy are vertically lined up. Above 10 MeV of excitation, each strong transition in the $^{27}Al(^3He,d)$ reaction matches with a transition seen in the $^{28}Si(p,p')$ reaction. States at 10.18, 11.59, 12.49, 12.64, 12.79, 13.12, 13.25, 13.72, 13.98, 14.10, and 14.37 MeV are excited in the $^{27}Al(^3He,d)$ reaction by clear $\ell_p = 3$ angular distributions. This indicates that these states have parts of the $(d_{5/2}, {}^{-1}f_{7/2})$ 1p - 1h configuration. Based on the assumption that the high spin members of this multiplet are quite pure, the (2J + 1) rule was applied to tentatively associate the spin and parity values of 5^-, 6^-, and 4^- with the states at 12.64, 13.25, and 14.37 MeV, respectively. The 6^- and 4^- states are near the positions predicted by Donnelly and Walker,[1,2] but the excitation energies do not agree well with those of state seen in the (e,e') experiment.[1]

REFERENCES

1. T.W. Donnelly, et al., Phys. Letters 32B, 545(1970).

2. T.W. Donnelly and G.E. Walker, Annals of Physics 60, 209(1970).

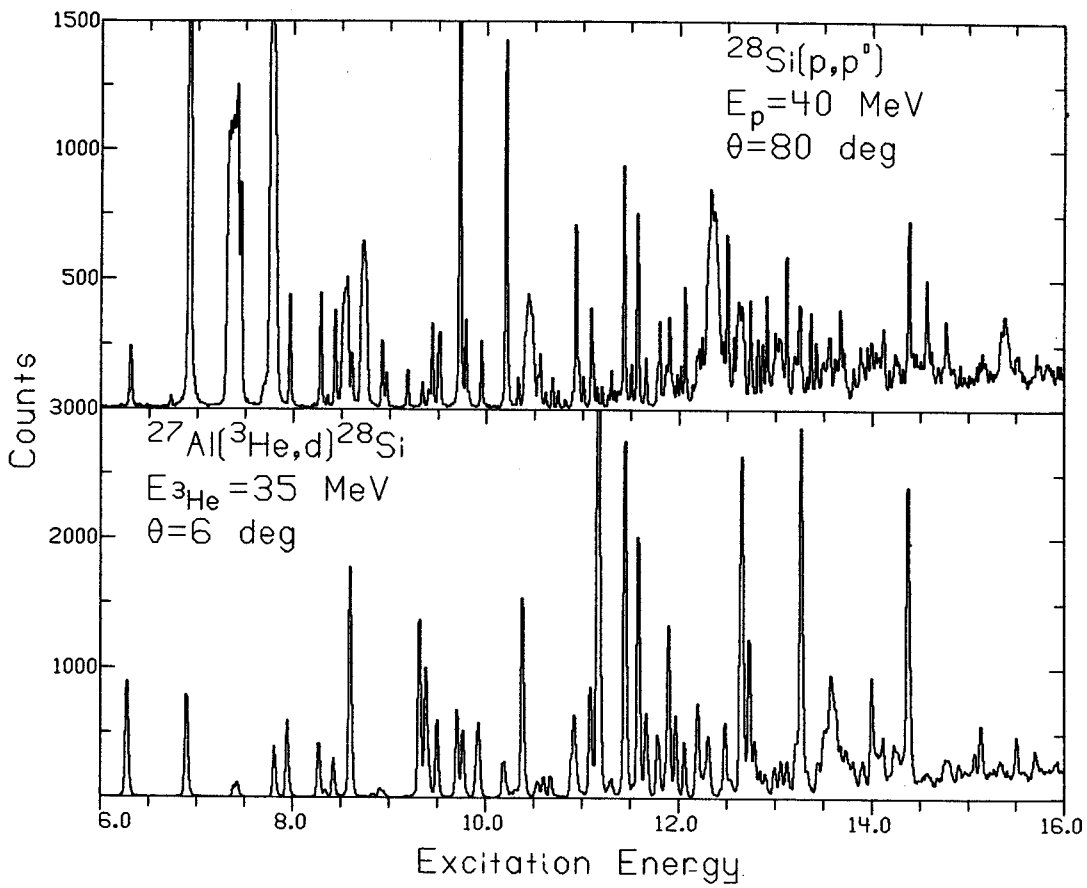

FIG. 1.--Sample spectra of states in ^{28}Si populated via the (p,p') and (^3He,d) reactions. They are plotted on a common excitation energy scale.

Elastic Neutron Scattering From ^{40}Ca

L.E. Young, S.D. Schery, R.R. Doering, R.K. Bhowmik, S.M. Austin, and R. DeVito

While there is much elastic proton scattering data from ^{40}Ca available for optical-model analysis, there is a substantial lack of accurate neutron elastic scattering data in the energy range available to the MSU neutron time-of-flight (TOF) facility. In this experiment angular distributions from the ^{40}Ca (n,n) ^{40}Ca reaction will be taken at several energies between twenty-five and forty-five MeV. The results will be used to provide information on the nucleon nucleus optical-model potential. In particular, the energy dependence will be investigated, and comparison with existing proton elastic scattering is expected to give precise information on the isospin-dependent part of the optical potential.

Differences in the optical-model potential felt by protons and neutrons are supposed[1] to originate mainly from terms dependent on projectile energy and neutron excess ($\frac{N-Z}{A}$). With the Z = N, ^{40}Ca target, the second effect is not present, making the analysis of the velocity dependence easier. This will be investigated by comparing measurements taken at differing projectile energies. The effect of velocity dependence can be reduced by modifying the neutron energy so that the average velocities of the neutron and proton projectiles are the same inside the nucleus. By using this "velocity matching" technique to compare neutron and proton data, this experiment will be sensitive to any breaking of charge symmetry in the nucleon-nucleus potential. Figure 1 shows the effect on the angular distribution of a 1 MeV charge in the strength of the central potential which is consistent with the magnitude of charge symmetry breaking proposed by Negele.[2]

This experiment utilizes a nearly monoenegetic beam of neutrons produced by the ^{7}Li (p,n)^{7}Be (0,0.429 MeV) reaction. A neutron flux of about 10^{7} n/cm^{2}/sec. can be obtained at the scattering sample. Because a beam swinger is used to vary the scattering angle, it is not difficult to insure good shielding along the direct path from the neutron production target to the fixed neutron detector.

A large area liquid scintillator (NE 224) detector is used, which provides pulse-shape-discrimination (PSD) information in addition to energy and TOF outputs. The data is collected using a versatile computer program (BKNTOF) which allows the setting of both energy thresholds and PSD gates on up to 8 TOF spectra. In order to insure proper subtraction of background, data are taken both with the scattering sample in and out (Fig. 2). Multiple scattering and geometrical affects from the finite size of the scattering sample are calculated with a Monte-Carlo program. It is expected that absolute cross sections will be determined to a few percent at forward angles. From the calculations shown in Fig. 1 it appears that the ratio of the cross section at the first maximum to that at the first minimum changes by eight percent for a 1 MeV change in the strength of the central potential. The present experiemnt should determine this ratio to better than a percent.

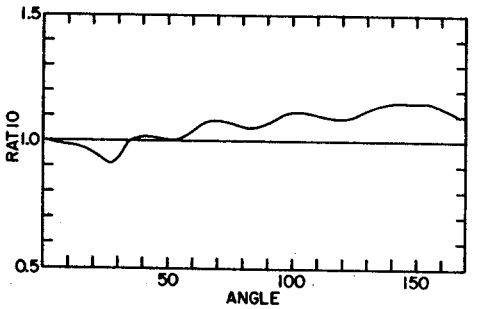

Fig. 1 Ratio of cross sections $\sigma(V_R=47.6$ MeV)/ $\sigma(V_R=46.6$ MeV) calculated for ^{40}Ca (n,n) at En = 30.3 MeV.

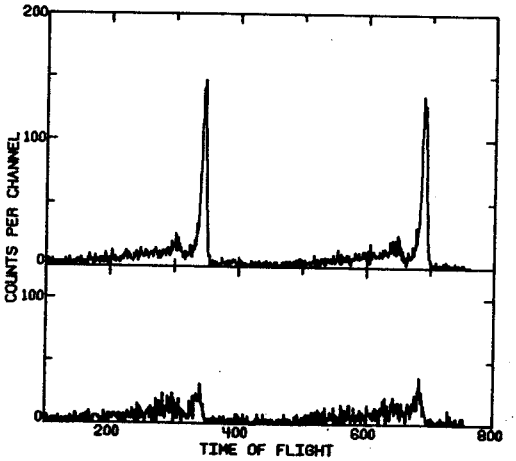

Fig. 2 The top histogram is the TOF spectrum obtained for ^{40}Ca (n,n) at E_N = 30.3 MeV and a 40° scattering angle. At the bottom is shown the background taken with the scattering sample removed.

REFERENCES

1. G.R. Satchler, p. 389 of Isospin in Nuclear Physics; ed. D.H. Wilkinson (North Holland, 1972).

2. J.W. Negele, Nucl. Phys. A165 (1971) 305.

Collective Model of Low-lying Monopole Excitations

H.P. Morsch and P. Decowski

Low-lying monopole excitations in (sd) and $f_{7/2}$ shell nuclei have been studied recently in a microscopic approach.[1] These strong monopole excitations may also be described in a rather simple collective picture in which the transition density is obtained using derivatives of the ground state density:

$$\rho_{tr} = \sum_{i=1}^{n} \frac{\partial \rho(x_1 \ldots x_n)}{\partial x_i}$$

Using a Woods-Saxon density $\rho(\rho_o,R,a)$, we obtain two different monopole excitation modes which may be given by:

$$\rho_1^{tr} = \delta\rho_o + \partial R\ \partial\rho/\partial R$$

and $$\rho_2^{tr} = \rho a \partial\rho/\partial a + \rho R\ \partial\rho/\partial R$$

with the constraint $\int \rho_{tr} d\tau = 0$ which is derived from the orthogonality of initial and final states. The first mode corresponds to the compressional mode of the nucleus whereas the second mode corresponds to a diffuseness oscillation. As the compressional mode of the nucleus is expected to be high in energy the low-lying monopole excitation may be discussed as a diffuseness oscillation.

This collective monopole description was applied to the excitation of the first 0^+ state in ^{24}Mg at 6.43 MeV. Fig. 1 shows the transition density corresponding to the two possible monopole modes (solid line-diffuseness oscillation, dashed line-compressional mode). The diffuseness oscillation yields a transition radius much larger than that of the compressional mode. This allows an experimental distinction between these two different modes, e.g., a transition radius of 4.9 fm and 6.0 fm is obtained for a compressional mode and the diffuseness oscillation, respectively. The experimental transition radius is 5.8 fm in good agreement with that of the diffuseness oscillation. Using this collective density a reasonable fit to our α obtained as is shown in Fig. 2.

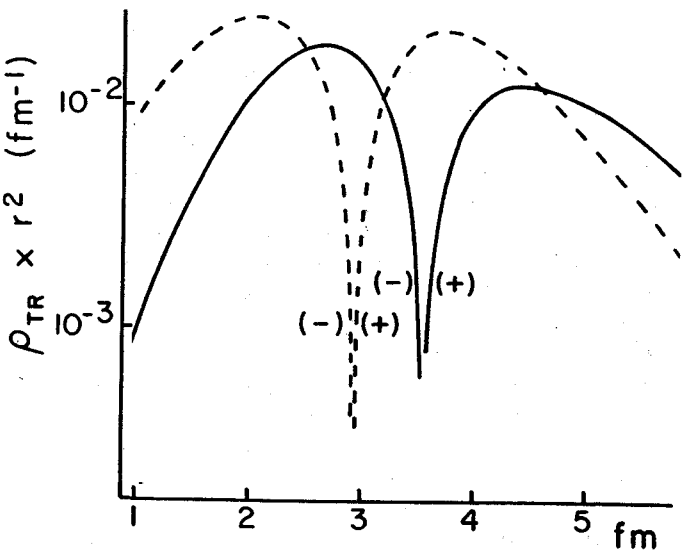

FIGURE 1

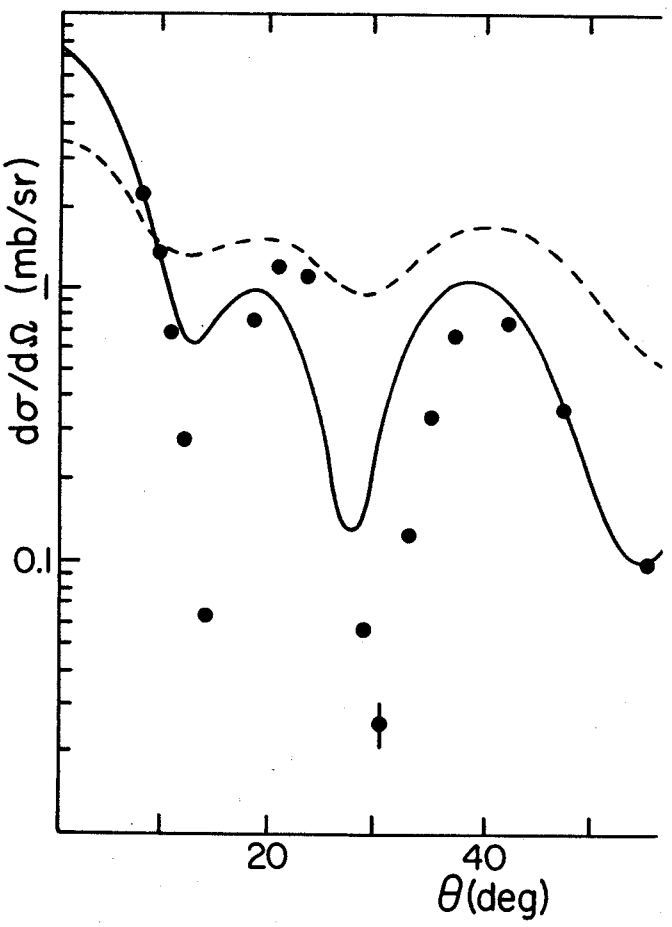

FIGURE 2

REFERENCES

1. H.P. Morsch, Nucl. Phys. A226(1974)506.

2. H.P. Morsch, Phys. Lett. 56B(1975)115

3. H.P. Morsch, D. Dehnhard and T.K. Li, Phys. Rev. Lett. 34(1975)1527.

Monopole Excitations in ^{12}C and ^{24}Mg

H.P. Morsch, P. Decowski and B.H. Wildenthal

Inelastic α scattering to first excited 0^+ states in ^{12}C and ^{24}Mg has been measured at E_α=40 MeV. For ^{24}Mg this transition has been studied previously[1] and a strong 1p shell hole structure has been found. The higher energy of this experiment is used for a sensitive test of the reaction mechanism. The comparison of this monopole transition with that in ^{12}C is of interest because the structure of these two transitions are expected to be rather different containing a large fraction of the Giant Monopole Excitation in the ^{12}C case whereas for sd shell nuclei such admixtures of the Giant Monopole state were found to be small[2]. For ^{24}Mg the experimental angular distribution together with that of ref. 1 are shown in Fig. 1. The lines represent DWBA calculations using the same microscopic monopole form factors (discussed in ref. 1) for both energies, these yield an excellent fit in shape and absolute strengths. A further crucial test of our approach provides the comparison with electron scattering in which E0 matrix element $\langle r^2 \rangle$ and transition radius R_{tr} are obtained. The results are summarized in table 1. Both E0 matrix element and transition radius from our transition desities are in excellent agreement with the electron scattering results. Ambiguities between different 1p-sd shell components have been found, different sets of transition amplitudes (a^+a) are given which yield comparable results. For ^{12}C a comparable fit as for ^{24}Mg is obtained, however, in addition to 1p-sd shell components a rather large fraction of the 1p1h excitation had to be assumed.

References

1. H.P. Morsch, D. Dehnhard and T.K. Li, Phys. Rev. Lett. 34(1975)1527 and 35(1975)192.

2. H.P. Morsch, Phys. Lett. 61B(1976)15.

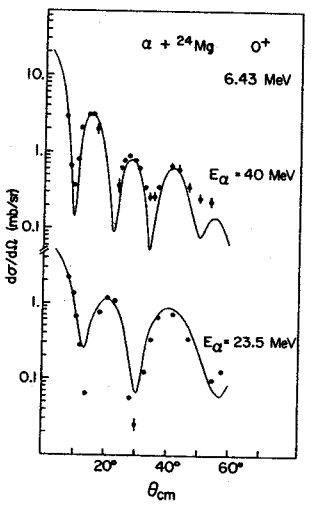

Figure 1.

TABLE 1

	^{4}HE SCATTERING $(a^+a)_{n,l,j}$								ELECTRON SCATTERING	
	$1p_{3/2}$	$1p_{1/2}$	$1d_{5/2}$	$2s_{1/2}$	$1d_{3/2}$	1p1h exc.	$\langle r^2 \rangle$ [fm^2]	R_{TR} [fm]	$\langle r^2 \rangle$ [fm^2]	R_{TR} [fm]
^{28}Si	-	-0.17	0.62	0.15	-0.60	-	6.94	6.34	6.8±0.4	5.7±0.5
^{24}Mg	-	-0.18 -0.87	0.50 0.43	0.33 0.44	-0.65 -	-	7.38 7.02	5.88 5.66	6.33±0.29	5.72±0.43
^{12}C	-0.28 -0.82	0.28 0.45	0.14 0.58	-0.14 -0.21	- -	70% 50%	5.75 5.60	4.37 4.37	5.37±0.22	4.24±0.30

Excitation of Collective Dipole Modes in ^{208}Pb

P. Decowski, H.P. Morsch and W. Benenson

Dipole excitations can exhibit strong collective features as observed for example in the isovector giant dipole resonance. Apart from this dipole excitation, isoscalar dipole and dipole spin-flip modes are also possible, both characterized by retarded electromagnetic transitions. However, they should be easily excited in inelastic scattering of strongly interacting particles. We have studied inelastic proton scattering from ^{208}Pb at 45 MeV. Also, in order to distinguish between isoscalar excitations and isovector or spin-slip excitations we have studied α scattering at 48 MeV. In the proton scattering we find in the excitation region 7-8.5 MeV a concentration of strong states with L=1 structure. Fig. 1 shows angular distributions of four of these states which could be well separated from the neighboring other peaks. A comparison with (γ,n) and (γ,γ')reactions shows that these states cannot be of normal isovector dipole structure: their relatively large cross sections would correspond to cross sections in (γ,n) and (γ,γ') at least 10 times larger than measured experimentally.

An isoscalar dipole assignment can be ruled out because these states are not excited in inelastic α scattering. However, a dipole spin-flip assumption is consistent with the experimental data. This excitation (L=1,S=1) forms a multiplet with spins 0^-, 1^-, 2^- and yields retarded electromagnetic transitions. Such interpretation is consistent with results from electron scattering[1] at 180° in which two of our states were identified as M2 excitations (leading to a spin 2^-). Other states in questions were identified as 1^- states[2,3]. The microscopic calculations in Fig. 1 yield a strength which exhausts about 60% and 20% of the isoscalar dipole spin-flip sum rule for 1^- and 2^- states respectively, and about 30% of the total dipole spin-flip strength. Calculations[4] find ∿50% of the (ΔT=0) + (ΔT=1) dipole spin-flip strength in the excitation region between 8-11 MeV.

In the α scattering experiment we observed three dipole states at 4.84, 5.28, 5.50 MeV which belong to the isoscalar dipole excitation. This excitation may be described in a collective model by a dipole diffuseness oscillation (quite similar to monopole excitations, see the section on "Inelastic scattering"). Using this collective transition density we get a good fit to the experimental data with a diffuseness change of 0.2 fm. (dashed curve in Fig. 2). In microscopic models this mode can be interpreted as dipole oscillations of nucleons with large angular momentum against nucleons with smaller angular momentum. The experimental data were compared with DWBA calculations using the shell model wavefunctions of ref. 5. Although the most collective low lying states of ref. 5 (calculated energies 4.96 5.97 and 5.27 MeV lines 1, 2 and 3 in Fig. 2, respectively) have been used the experimental cross sections are underpredicted by one order of magnitude. This indicates a dipole excitation with a high degree of collectivity that cannot be described by a $1\hbar\omega$ excitation only.

REFERENCES

1. R.A. Lindgren et al., Phys. Rev. Lett. 35 (1975) 1423.
2. R.J. Holt and H.E. Jackson, Phys. Rev. Lett. 36 (1976) 244.
3. E.D. Earle et al., Phys. Lett. 32B (1970) 471.
4. M. Harvey and F.C. Khanna, Nucl. Phys. A221 (1974) 77.
5. W.W. True et al., Phys. Rev. C3 (1971) 2421.

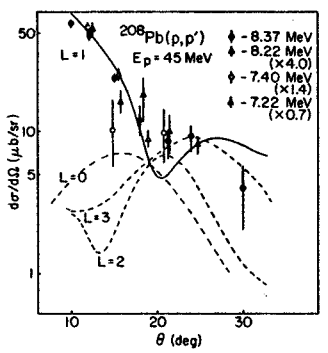

FIGURE 1

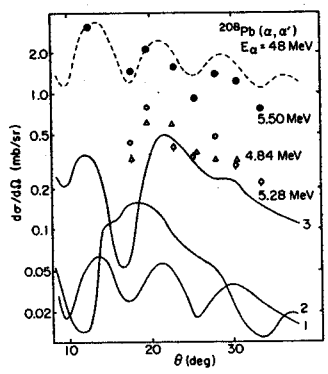

FIGURE 2

Fine Structure in the Giant Resonance Region of ^{208}Pb

H.P. Morsch, P. Decowski and W. Benenson

Inelastic scattering of 45 MeV protons has been used to study the giant resonance region of ^{208}Pb. The scattered particles were detected in a delay line counter in the focal plane of the Enge Split pole Spectrometer. The raw proton spectra are shown in Fig. 1. Gross structures (width of 300 keV or more) similar to those observed in electron and proton scattering [1-3] are seen. In addition to the gross structure a strong fine structure is observed in the giant resonance region. It is interesting to note that the fine structure peaks show distinct differences in their angular dependence, which implies the excitation of different multipolarities. There are peaks which show up mainly at forward angles indicated by cross hatching in the 12° spectrum. There are also other peaks which are dominant at larger angles, e.g. at 9.35 and 10.3 MeV. The angular distributions of some of the states with characterstics angle dependence are shown in Fig. 2 together with DWBA predictions using microscopic form factors. Details of these calculations together with a discussion of the monopole excitation at 9.11 MeV are given in ref. 4.

A monopole excitation at 8.9 MeV (50% of the sum rule strength) has been proposed in ref. 5. Such a strong monopole state has not been seen in our experiment. Instead we find in this region many peaks of quadrupole character. We conclude that the structure observed in ref. 5 consists mainly of quadrupole states, as suggested in ref.6.

References

1. F.R. Buskirk, et al., Phys. Lett. 42B(1972)194.
2. M. Nagao and Y. Torizuka, Phys. Rev. Lett. 30 (1973) 1068.
3. M.B. Lewis, F.E. Bertrand and D.L. Horen, Phys. Rev. 8(1973)398.
4. H.P. Morsch, P. Decowski and W. Benenson, Phys. Rev. Lett. 37(1976)263.
5. R. Pitthan, et al., Phys. Rev. Lett. 33(1974) 849.
6. A. Schwierczinski, et al., Phys. Rev. Lett. 35 (1975) 1244.

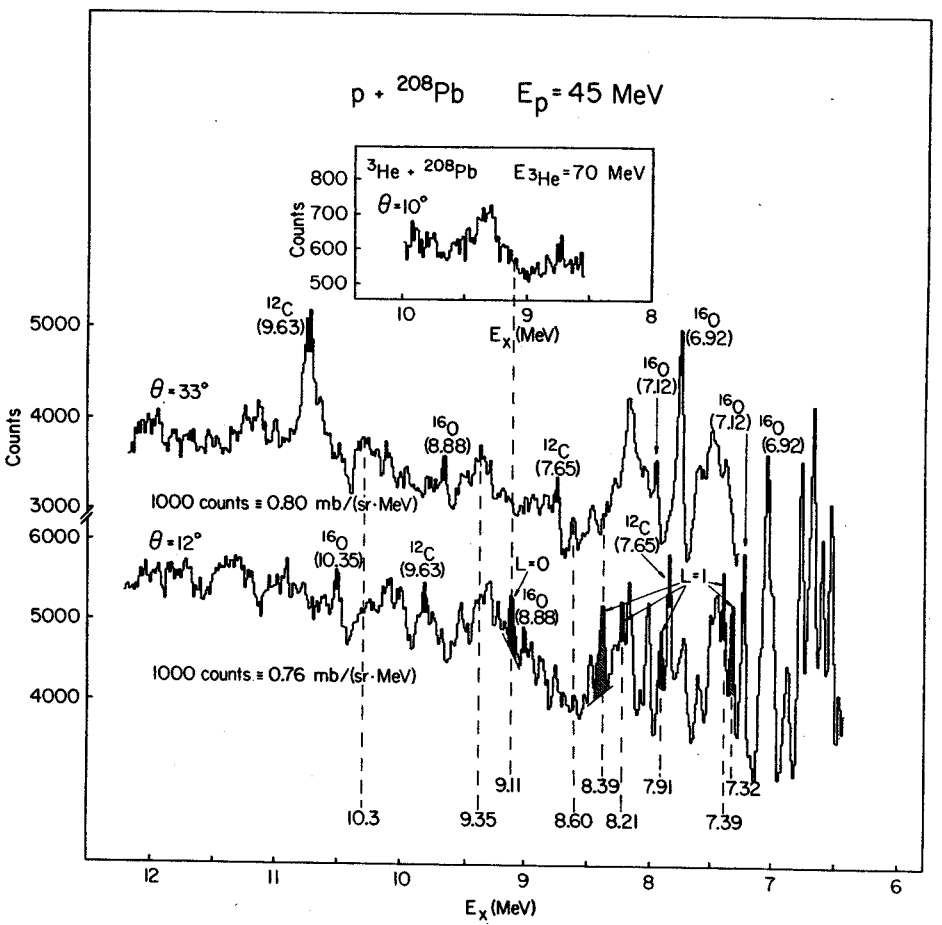

Figure 1

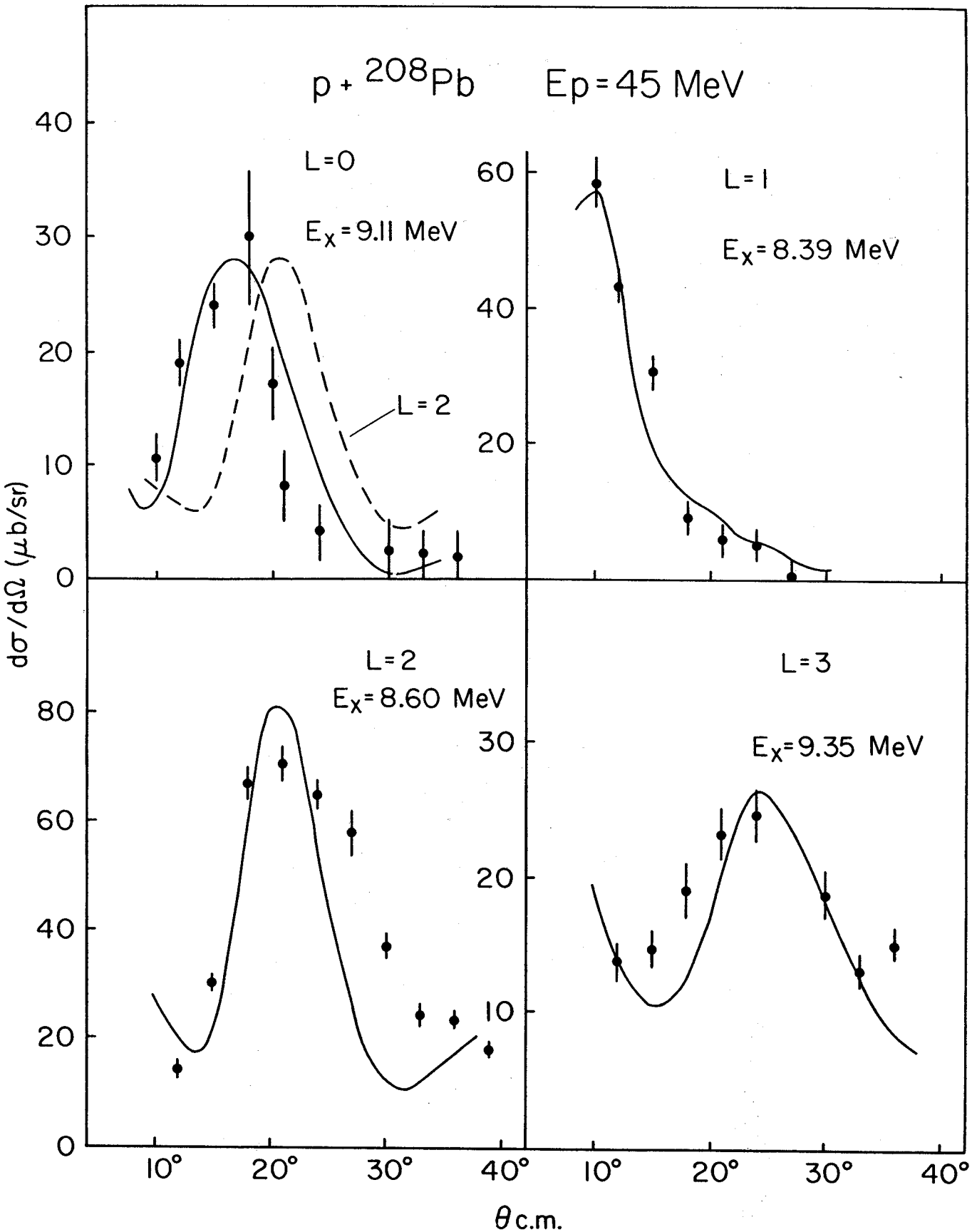
p + 208Pb Ep = 45 MeV
L=0
Ex = 9.11 MeV
L=2
L=1
Ex = 8.39 MeV
L=2
Ex = 8.60 MeV
L=3
Ex = 9.35 MeV
dσ/dΩ (μb/sr)
θ c.m.
10°
20°
30°
40°

Figure 2